Metabolic Engineering 67 (2021) 29–40

Contents lists available at ScienceDirect

Metabolic Engineering

journal homepage: www.elsevier.com/locate/meteng

Engineering adipic acid metabolism in *Pseudomonas putida*

Yannic S. Ackermann [a,1], Wing-Jin Li [b,1], Leonie Op de Hipt [a], Paul-Joachim Niehoff [b], William Casey [c], Tino Polen [a], Sebastian Köbbing [b], Hendrik Ballerstedt [b], Benedikt Wynands [a], Kevin O'Connor [d,e], Lars M. Blank [b], Nick Wierckx [a,*]

[a] Institute of Bio- and Geosciences IBG-1: Biotechnology, Forschungszentrum Jülich, Jülich, Germany
[b] Institute of Applied Microbiology - iAMB, Aachen Biology and Biotechnology - ABBt, RWTH Aachen University, Aachen, Germany
[c] Bioplastech Ltd., NovaUCD, Belfield Innovation Park, University College Dublin, Dublin, Ireland
[d] UCD Earth Institute and School of Biomolecular and Biomedical Science, University College Dublin, Dublin, Ireland
[e] BiOrbic Bioeconomy SFI Research Centre, University College Dublin, Dublin, Ireland

ARTICLE INFO

Keywords:
Plastic upcycling
Adipic acid
Pseudomonas putida
Polyhydroxyalkanoate
Metabolic engineering
Metabolic network

ABSTRACT

Bio-upcycling of plastics is an upcoming alternative approach for the valorization of diverse polymer waste streams that are too contaminated for traditional recycling technologies. Adipic acid and other medium-chain-length dicarboxylates are key components of many plastics including polyamides, polyesters, and polyurethanes. This study endows *Pseudomonas putida* KT2440 with efficient metabolism of these dicarboxylates. The *dcaAKIJP* genes from *Acinetobacter baylyi*, encoding initial uptake and activation steps for dicarboxylates, were heterologously expressed. Genomic integration of these *dca* genes proved to be a key factor in efficient and reliable expression. In spite of this, adaptive laboratory evolution was needed to connect these initial steps to the native metabolism of *P. putida*, thereby enabling growth on adipate as sole carbon source. Genome sequencing of evolved strains revealed a central role of a *paa* gene cluster, which encodes parts of the phenylacetate metabolic degradation pathway with parallels to adipate metabolism. Fast growth required the additional disruption of the regulator-encoding *psrA*, which upregulates redundant β-oxidation genes. This knowledge enabled the rational reverse engineering of a strain that can not only use adipate, but also other medium-chain-length dicarboxylates like suberate and sebacate. The reverse engineered strain grows on adipate with a rate of $0.35 \pm 0.01\ h^{-1}$, reaching a final biomass yield of $0.27 \pm 0.00\ g_{CDW}\ g_{adipate}^{-1}$. In a nitrogen-limited medium this strain produced polyhydroxyalkanoates from adipate up to 25% of its CDW. This proves its applicability for the upcycling of mixtures of polymers made from fossile resources into biodegradable counterparts.

1. Introduction

Production of plastics reached 359 million tons in 2018 and is almost completely based on fossil resources. By 2050 the plastics industry will have produced an average of 500 million tonnes per year consuming 20% of total oil production (World Economic Forum, 2016; Geyer et al., 2017). Plastics have a wide range of advantageous properties such as flexibility, durability, and light weight. However, most plastics are extremely stable, and without good end-of-life management they will accumulate in all major terrestrial and aquatic ecosystems on the planet (Andrady and Neal, 2009; Narancic et al., 2018; PlasticsEurope, 2019). The pollution of plastic has recently been highlighted as a global crisis at every stage, from production to disposal and incineration (RameshKumar et al., 2020).

Ideally, a fully circular economy is realized where all plastic is recycled with no leakage to the environment. However, this is unrealistic, and surely far from the current reality, in which only a small fraction of plastics is recycled (PlasticsEurope, 2019). Even if all waste would be collected, a lack of economically viable recycling options for many plastic waste streams currently limits useful retention of carbon in the cycle. There is therefore a strong need for new technologies especially for the recycling of impure mixed waste streams, as well as for thermoset polymers like polyurethane foams that are not amenable to mechanical recycling. In addition, wear and tear of microplastics from, e.g. tire friction or washing will invariably lead to a certain level of environmental pollution. One possible way to ameliorate the problem of

* Corresponding author.
E-mail address: n.wierckx@fz-juelich.de (N. Wierckx).
[1] these authors contributed equally to this study.

https://doi.org/10.1016/j.ymben.2021.05.001
Received 11 February 2021; Received in revised form 12 April 2021; Accepted 1 May 2021
Available online 7 May 2021

plastic pollution is the development of biodegradable polymers. These likely remain in the environment for a shorter time, although environmental degradation should always be considered an "emergency" last resort (Wei et al., 2020).

The development of chemical (Meys et al., 2020; Rorrer et al., 2019; Vollmer et al., 2020) and biological (Narancic et al., 2020; Wei et al., 2020) plastic depolymerization processes has recently enabled a qualitatively new way of recycling. Major advances have been made in the depolymerization of polyesters (Knott et al., 2020; Tournier et al., 2020; Westhues et al., 2018), polyurethanes (Magnin et al., 2020) and polyamides (Kumar et al., 2020). Biodegradable polymers, like polyhydroxyalkanoate (PHA) and polybutylene adipate terephthalate (PBAT) are especially amenable to this approach, since they are by definition easier to depolymerize. In the case of mixed waste streams, depolymerization of plastic waste will yield a complex mixture of plastic monomers with terminal alcohol, carboxylic acid, and amine groups, the separation and purification of which may not always be economical. In this case, biological funneling is a powerful approach to convert plastic hydrolysates into value-added chemicals (Kim et al., 2019; Tiso et al., 2021; Utomo et al., 2020). This bio-upcycling of plastics has recently been heralded as a promising new approach to waste management (Wierckx et al., 2015).

A prerequisite for the biological funneling of plastic hydrolysates is the efficient microbial metabolism of the contained monomers. In this respect, Pseudomonads are considered highly promising microbial catalysts (Wierckx et al., 2015; Wilkes and Aristilde, 2017). Different non-pathogenic strains of this genus possess favorable intrinsic properties such as high tolerance to chemical stresses and fast and efficient growth (Heipieper et al., 2007; Nikel and de Lorenzo, 2018; Schwanemann et al., 2020; Volmer et al., 2014; Wynands et al., 2019). The last decade has also seen an explosion of available genetic tools (Aparicio et al., 2019; Köbbing et al., 2020; Martínez-García and de Lorenzo, 2011; Nikel et al., 2014; Zobel et al., 2015), enabling deep metabolic engineering for efficient bioproduction (Lenzen et al., 2019; Otto et al., 2019) and the generation of streamlined chassis strains (Nikel and de Lorenzo, 2018; Shen et al., 2017; Wynands et al., 2019). Pseudomonads are also well known for their metabolic versatility, which already enabled growth on a variety of plastic monomers. *P. putida* KT2440 was naturally capable of growing on diols like ethylene glycol and 1,4-butanediol, but this ability needed to be activated or enhanced by metabolic and/or evolutionary engineering (Li et al, 2019, 2020). Several natural isolates are further capable of degrading styrene (Baggi et al., 1983), terephthalate (Narancic et al., 2021), and 2,4-toluenediamide (Espinosa et al., 2020). One class of compounds that so far cannot be metabolized by Pseudomonads are medium-chain-length (mcl)-dicarboxylates like adipic or sebacic acid.

Adipic acid and other mcl-α,ω-dicarboxylates are mainly used in the production of polyamides, polyesters, and polyurethanes. Adipic acid is industrially produced from fossil benzene (Sato, 1998), but several microbial production methods have also been developed (Chae et al., 2020). Lipids, lignin, and (hemi-)cellulose-derived feedstocks can be utilized to produce muconic or glucaric acid (Bentley et al., 2020; Otto et al., 2020; Salvachúa et al., 2018), which can subsequently be converted to adipic acid *via* catalytic hydrogenation (Cheong et al., 2016; Kohlstedt et al., 2018; Kruyer and Peralta-Yahya, 2017; Vardon et al., 2015). Further, *E. coli* strains have been developed that can convert glucose directly into adipic acid (Polen et al., 2013; Zhao et al., 2018). This biosynthesis pathway utilizes a reverse β-oxidation route that is similar to the degradation route for adipic acid (Kallscheuer et al., 2017). Microbial degradation of adipic acid and other mcl-dicarboxylates was characterized in *Acinetobacter baylyi* (Parke et al., 2001), a robust and versatile Gram-negative soil bacterium used for characterization, evolution, and engineering of enzymes and metabolic pathways (Barbe et al., 2004; Pardo et al., 2020; Tumen-Velasquez et al., 2018). In this species, adipic acid is first activated to adipyl-CoA, after which it is further metabolized *via* β-oxidation. The responsible genes are clustered in two operons. One encodes enzymes for the transport (DcaK and DcaP), CoA transferase subunits (DcaIJ), and an acyl-CoA dehydrogenase (DcaA). The other operon (*dcaECHF*) encodes enzymes related to β-oxidation including an enoyl-CoA hydratase, ketoacyl-CoA reductase, hydroxyl-CoA dehydrogenase, and a thiolase (Fischer et al., 2008) (Fig. 1).

In this work, the substrate spectrum of *P. putida* KT2440 is expanded to encompass mcl-dicarboxylates like adipic acid. Initial metabolic uptake and activation steps are heterologously inserted using genes from *A. baylyi*, followed by adaptive laboratory evolution to enable and enhance growth. The resulting strains are analyzed by genome resequencing and the adipate-metabolizing phenotype is reverse engineered in the wild type. The resulting strains grow at a rate of $0.31 \pm 0.02\ h^{-1}$ on adipic acid as sole carbon source, and they can also metabolize other mcl-dicarboxylates like suberic, azelaic, and sebacic acid.

2. Results and discussion

2.1. Enabling adipate metabolism by P. putida KT2440

Initial growth experiments showed that *P. putida* KT2440 is unable to metabolize adipate as sole carbon source, even after prolonged incubation. *In silico* comparison of the *P. putida* KT2440 genome to the adipate metabolic enzymes from *A. baylyi* (Parke et al., 2001) indicated a partial overlap with the 4-hydroxybenzoate and phenylacetate degradation pathways, starting at the level of 2,3-didehydroadipyl-CoA and 3-oxoadipyl-CoA, respectively (Fig. 1). There are no known *P. putida* homologs of DcaIJ and DcaA. However, a BLAST search with DcaA yielded several hits with putative acyl-CoA dehydrogenases with up to 40% sequence identity, and the sequences of DcaIJ are 66% and 62% identical to the 3-oxoadipyl-CoA transferase PcaIJ of *P. putida* KT2440. The *pcaIJ* genes are induced by 3-oxoadipate or indirectly by 4-hydroxybenzoate in *P. putida* ATCC12633 (Ornston and Parke, 1976; Parales and Harwood, 1993). These metabolites also induce a 3-oxoadipate uptake system that enables adipate import, likely encoded by *pcaT*. However, the same studies also confirm the initial observation that in spite of this, neither the wild-type *P. putida* ATCC12633, nor constitutive transporter mutants, grow on adipate as sole carbon source. Therefore, the *dcaAKIJP* operon from *A. baylyi*, encoding the adipyl-CoA transferase, dehydrogenase, and putative adipate uptake proteins, was overexpressed on vector pBNT-*dcaAKIJP*.

In theory, this overexpression completes the genetic inventory of *P. putida* for the metabolism of adipate. However, the resulting *P. putida* KT2440 pBNT-*dcaAKIJP* did not grow on adipate as sole carbon source. This may be attributed to a lack of induction of the native genes encoding the downstream 2,3-didehydroadipyl-CoA metabolic pathway. A similar phenomenon was observed for *P. putida* incubated with ethylene glycol (Li et al., 2019). Growth on this substrate was enabled by the addition of the upstream metabolite allantoin, which activated a glyoxylate metabolic pathway fed by the oxidation of ethylene glycol. This misregulation was abolished through adaptive laboratory evolution (ALE), which resulted in mutations that constitutively activated the pathway. We therefore subjected *P. putida* KT2440 pBNT-*dcaAKIJP* to ALE, using a co-feeding scheme of adipate and supporting carbon sources glucose and 4-hydroxybenzoate. 4-Hydroxybenzoate was used to induce the abovementioned *pcaIJ* and *pcaE*, as well as genes like *pcaF-I* and *pcaF-II via* its metabolites protocatechuate and 3-oxoadipate (Parales and Harwood, 1993). The latter genes are involved in the degradation of the common intermediate 3-oxoadipyl-CoA (Fig. 1). A stepwise increase in adipate and decrease of supporting carbon sources was used to evolve *P. putida* KT2440 with pBNT-*dcaAKIJP* in two individual batches (Fig. 2). No salicylate was added as inducer of the NagR/P_{nagAa} promoter system, which controls the *dcaAKIJP* operon, relying instead on leaky expression of the promoter. This omission provides higher selective pressure on gain-of-function mutations in

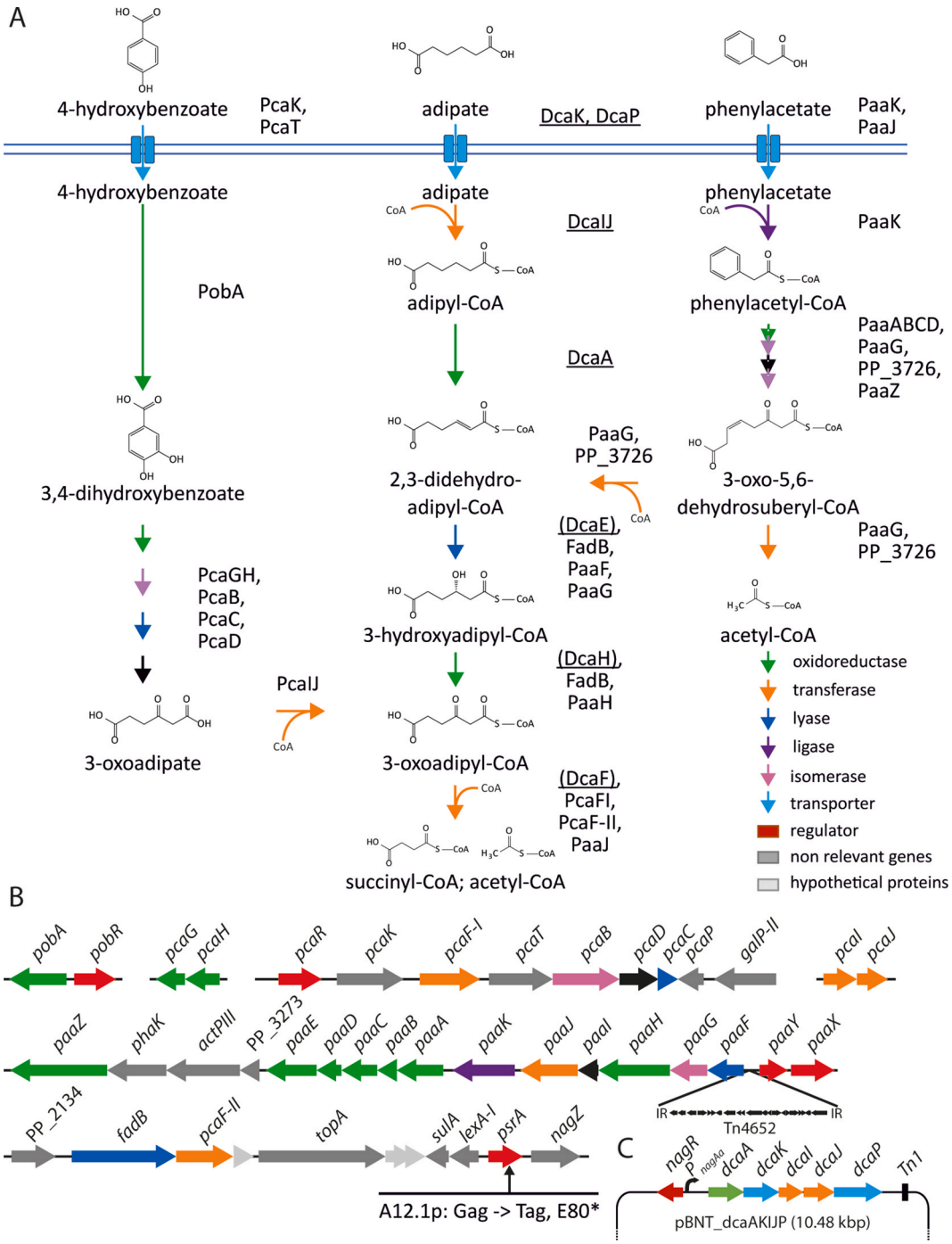

Fig. 1. Overview of genes and enzymes involved in adipate metabolism. A) Comparison of the adipate metabolic pathway of *A. baylyi* (underlined proteins) with the 4-hydroxybenzoate and phenylacetate pathways from *P. putida* KT2440. Annotations refer to top-level EC classes. **B)** Genomic organization of genes encoding 4-hydroxybenzoate and phenylacetate pathway enzymes in *P. putida* KT2440. Colors correspond to the encoded enzymes in **A**. Discovered mutations in ALE strains are shown below the relevant genes. **C)** Plasmid-based expression cassette of *dcaAKIJP*. (For interpretation of the references to colour in this figure legend, the reader is referred to the Web version of this article.)

native genes similar to the heterologously expressed operon, as previous work indicated that an adipate-metabolizing strain might be evolved without the plasmid (Ornston and Parke, 1976).

When glucose was supplemented to medium 1 (Fig. 2B), the strain grew overnight. The second overnight culture was washed in MSM buffer and used to inoculate medium 2 with 4-hydroxybenzoate and adipate as carbon sources. Growth phases increased to two days reaching OD_{600} 2.6–3.5 and could be shortened after three transfers to one day. When 1 mM 4-hydroxybenzoate was co-fed with 20 mM adipate (medium 3) in the A12p culture, optical densities of only 0.16 were reached. This strongly indicates that up to this point adipate was not metabolized. A drastic change was observed after four transfers, which were performed by harvesting the cells and transferring them to fresh medium 3. Subsequent cultures reached high OD_{600} values, which could only be achieved through adipate utilization. The resulting evolved population grew overnight to an OD_{600} of 3.6 on adipate as sole carbon source. Eighty-four strains from evolved cultures were isolated on LB agar plates and tested for growth on adipate (Fig. 2). The fastest growing strains from each batch were selected and called A6.1p and A12.1p (first strain evolved on adipate with 6 or 12 sequential batches harboring a

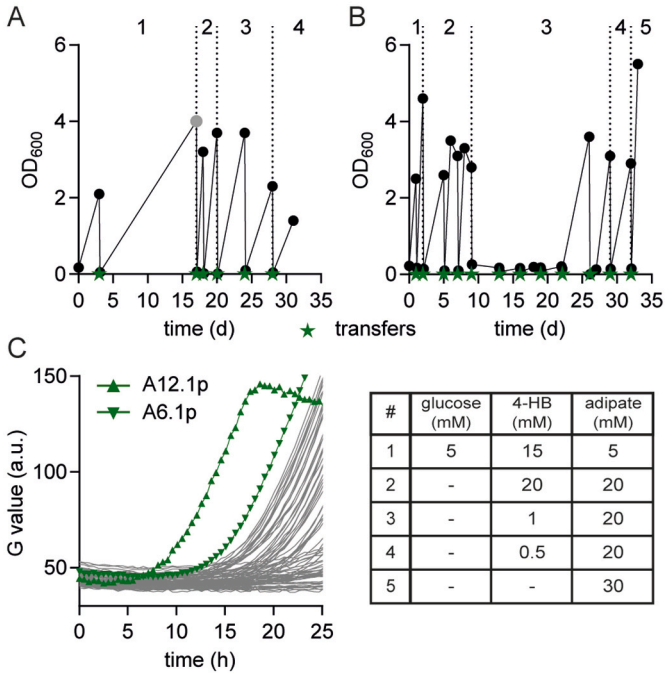

#	glucose (mM)	4-HB (mM)	adipate (mM)
1	5	15	5
2	-	20	20
3	-	1	20
4	-	0.5	20
5	-	-	30

Fig. 2. Adaptive laboratory evolution of *P. putida* KT2440 pBNT-*dcaAKIJP* on adipate. Sequential batch cultivation to obtain the evolved populations A6p (**A**) and A12p (**B**) on MSM medium with the substrate concentrations as indicated in the legend (4-HB: 4-hydroxybenzoate). The greyed symbol is an estimated value after visual inspection of a long-term cultivation. **C**) Growth of 84 single strains isolated from the two ALE batches in two-fold buffered MSM with kanamycin and 30 mM adipate. The strains A12.1p (▲) and A6.1p (▼) were selected for further investigation. Growth was detected *via* a Growth Profiler® using a 96-well plate. (For interpretation of the references to colour in this figure legend, the reader is referred to the Web version of this article.)

plasmid). Both strains had retained plasmid pBNT-*dcaAKIJP* and were kanamycin resistant. In MSM with kanamycin, 0.1 mM salicylate as inducer, and 30 mM adipate as sole carbon source, strain A12.1p grew at a rate of $0.29 \pm 0.00\ h^{-1}$, which is 2.8-fold faster than A6.1p which grew at a rate of $0.11 \pm 0.00\ h^{-1}$.

2.2. Genome sequencing of evolved adipate-metabolizing strains

To understand the molecular basis of the phenotype of the two evolved strains and their plasmids, genome re-sequencing was conducted. Sequencing data are deposited in the NCBI Sequence Read Archive under BioProject number PRJNA464914 with accession numbers SRX9220792 for A6.1p and SRX9220793 for A12.1p. In total 51 mutations were found in A6.1 and 53 mutations in A12.1. As was shown previously for sequenced strains evolved on ethylene glycol and 1,4-butanediol, most of the genomic mutations are also present in our laboratory wild type and therefore unlikely to contribute to adipate metabolism (Li et al, 2019, 2020). Of the remaining mutations (Table 1), one prominent phenomenon stood out in both evolved strains. The sequence read coverage for transposon Tn4652 was twice as high as the average genomic coverage. This transposon is known to be activated under stress conditions such as starvation (Ilves et al., 2001). It was previously found to play a role in ALE-derived strains growing on ethylene glycol and 1,4-butanediol (Li et al, 2019, 2020). It contains a predicted promoter at its 3′-end and is known for generating novel fusion promoters upon insertion into a new locus (Nurk et al., 1993; Teras et al., 2000). Arbitrary-primed PCR revealed that this transposon had replicated into a second locus, between *paaFGHIJ* and *paaYX*. The *paa* cluster encodes enzymes responsible for the degradation of phenylacetate, which shows parallel activities to adipate degradation (Fig. 1). In *E.coli*, PaaX is a repressor of *paaZ* and *paaABCDEFGHIJK* (Fernández et al., 2014). Phenylacetate is CoA-activated to phenylacetyl-CoA, which binds to PaaX thereby releasing the repression by disassociating from the promoter binding site of P_Z and P_A (Ferrández et al., 2000). The function of PaaY is so far not fully understood. It is thought to inactivate PaaK, the phenylacetate-CoA ligase, by acetylation (Teufel et al., 2010).

Additionally, only identified in A12.1p, the *psrA* gene encoding a

Table 1
Genomic loci affected by ALE in A6.1p and A12.1p.

Found in strain	affected locus	putative function	mutation (position in genome)	putative effect	Reference
A6.1p, A12.1p	PP_0278	small hypothetical protein	insertion_-_T (336124^336125)	frameshift	Belda et al. (2016); Nelson et al. (2002)
A12.1p	PP_2144	TetR family transcriptional regulator (236 aa)	G→T (2445964)	nonsense E80*	Fonseca et al. (2014); Kang et al. (2008)
A6.1p, A12.1p	PP_2589	aldehyde dehydrogenase	C→T (2958523)	A428V	Kurihara et al. (2005)
A12.1p	PP_3988	hypothetical protein	deletion_T_- (4498312)	frameshift	Belda et al. (2016); Nelson et al. (2002)
A6.1p, A12.1p	PP_5037	lipocalin family lipoprotein	C→T (5740555)	S175N	Bishop (2000); Flower et al. (2000)
A6.1p, A12.1p	Tn4652	transposon	17 kb insertion (3719504^3719505)	promoter mutation	Ilves et al. (2001); Teras et al. (2000)

TetR family transcriptional regulator was mutated (GAG → TAG; E80*). This protein is a homolog to PsrA of *P. aeruginosa* (protein sequence identity of 85%), which is a global regulator of β-oxidation that, among others, represses *fadAB* (Fonseca et al., 2014; Kang et al., 2008). Since *pcaF-II* and *fadB* are close to *psrA*, and these also have high homologies to *fadAB* in *P. aeruginosa*, it is likely that they are also regulated by this transcriptional repressor, and that its disruption activates the expression of these genes (Fig. 1). Although *pcaIJ* were induced by 4-hydroxybenzoate during the ALE experiments, no mutations were found in their genomic region. A third mutation found only in A12.1p consists of a frameshift deletion in PP_3988, which affects the last 118 out of the total 682 amino acids of the encoded hypothetical protein of unknown function. However, restoring the wild-type sequence in A12.1 did not affect the growth of this strain on adipate, making it unlikely to be foundational to the phenotype of this strain (Fig. S1). Three further mutations were found in both strains (Table 1), but these were also deemed of lower priority due to their marginal putative effect or the lack of any apparent relation to adipic acid metabolism.

Besides genomic mutations, the plasmid of A6.1p contained one missense mutation in the *rep* gene, which encodes the replication initiator protein of the plasmid (Krüger et al., 2014). Mi et al. (2016) found similar mutations in the *rep* gene of a related pBBR1 plasmid backbone after ALE with *P. putida*, leading to a lower plasmid copy number which eliminated a plasmid-induced growth defect. Sequence read coverage analysis shows that the plasmid copy number in A6.1p is approximately 3-fold lower than in A12.1p (Fig. 3). Thus, the mutation in the *rep* gene of pBNT-*dcaAKIJP* of A6.1p likely reduces the expression of the *dca* operon.

2.3. Characterization of plasmid effects in evolved adipate-metabolizing strains

The effect of the mutation in the *rep* gene of the plasmid from A6.1p was investigated by curing the two evolved strains from their plasmids and re-transforming them with plasmids isolated from both strains (Fig. 3A). In the case of A12.1 there is a slight negative effect on growth on adipate from the re-transformation with its own plasmid (0.26 ± 0.01 h^{-1}) compared to the original evolved strain (0.29 ± 0.00 h^{-1}). The growth rate is significantly lower (0.22 ± 0.00 h^{-1}) if the plasmid from A6.1p is used. The opposite effect can be seen in A6.1, whose growth rate increases significantly with the plasmid from A12.1p (0.12 ± 0.00 h^{-1}) compared to the original evolved strain (0.11 ± 0.00 h^{-1}) and the re-transformed strain (0.10 ± 0.00 h^{-1}). However, the A6.1 strain with the plasmid of A12.1 still grew much slower than any of the A12.1 transformants, indicating the effect of additional genomic mutations in the A12 strain background on growth. Omission of salicylate as inducer of the *nagR*/P_{nagAa} promoter led to much slower growth compared to induced cultures (Fig. 3A). It thus seems that the omission of salicylate in the ALE provided insufficient selective pressure for the emergence of mutations that increased expression or led to gain-of-function of other genes.

The mutation in the *rep* gene likely relates to general plasmid instability issues during ALE, as shown by Mi et al. (2016), rather than to efficient growth on adipate. In order to avoid the influence of plasmid instability and copy number effects, we therefore opted to integrate the *dcaAKIJP* operon into the genome of *P. putida*. By excluding the variable copy number of the plasmid, the reproducibility and stability of the strain would increase. As additional advantage, no antibiotic selection is needed, thereby providing less metabolic burden. The constitutive synthetic promoter P_{14e} (Zobel et al., 2015) was used to drive the expression of the *dca* operon, making salicylate induction unnecessary.

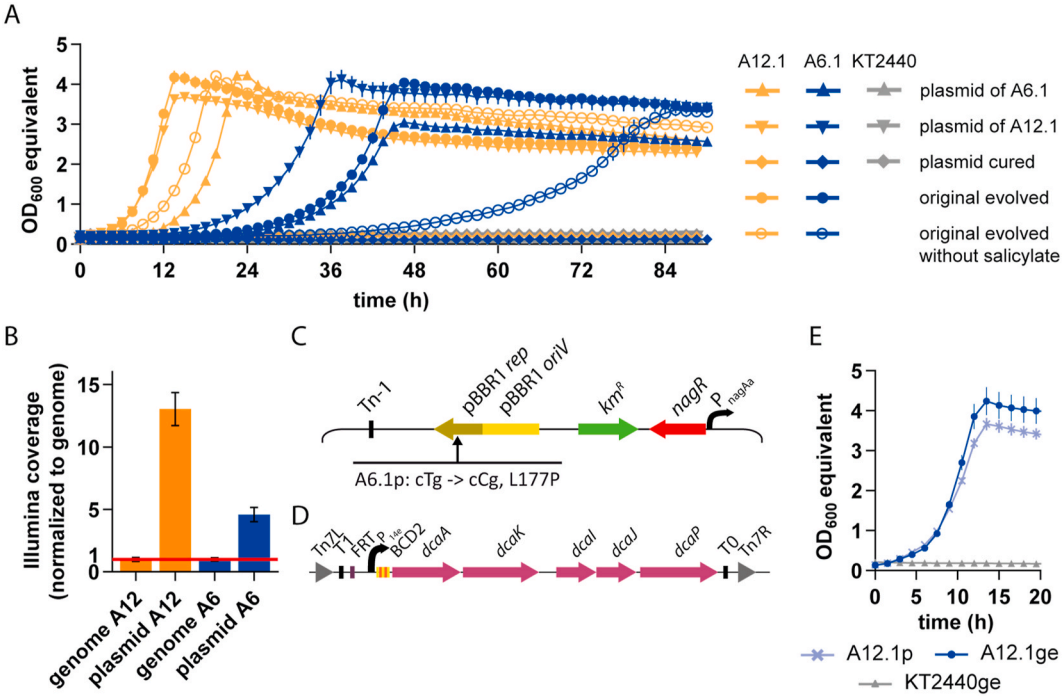

Fig. 3. Analysis of evolved pBNT-*dcaAKIJP* expression constructs. A) Comparison of growth on adipate of strains A12.1 (orange) and A6.1 (blue) with and without the indicated plasmids. Open symbols indicate omission of salicylate. **B**) The average sequence read coverage of the plasmids normalized to the genome. **C**) Mutation in the backbone of plasmid pBNT-*dcaAKIJP*. **D**) Mini-Tn7 genomic integration construct for constitutive expression of *dcaAKIJP*. **E**) Growth curves of *P. putida* A12.1 with episomal and genomic expression of the *dcaAKIJP* genes. Growth curves were measured in MSM with 30 mM adipate with the Growth Profiler and the results were converted to an equivalent OD at 600 nm. Error bars indicate the standard error of the mean (n = 3 (A), n = 5 (E)). (ge = genomically integrated P_{14e}-*dcaAKIJP;* p = pBNT-*dcaAKIJP*). (For interpretation of the references to colour in this figure legend, the reader is referred to the Web version of this article.)

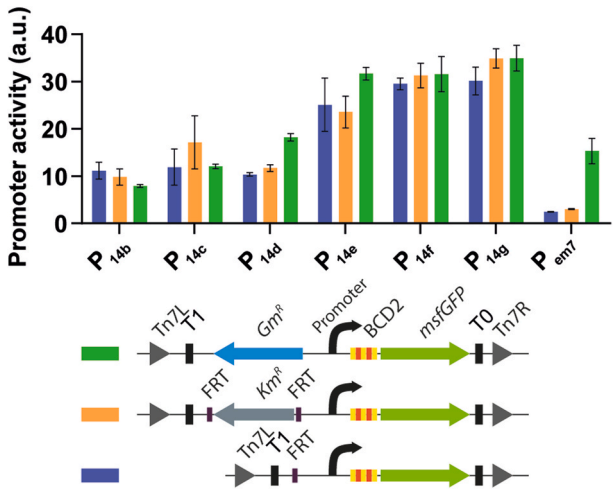

Fig. 4. Characterization of genomically integrated mini-Tn7 marker recycling constructs in *P. putida* KT2440. The original construct containing a Gm^R marker (green bars) is compared with new versions containing a recyclable Km^R marker flanked by two FRT sites, before (orange bars) and after (blue bars) marker recycling. Strains were cultured in a BioLector in minimal medium with 20 mM glucose in a 96 well plate. Identical strains from at least three different transformations were tested, with three biological replicates each. Promoter activity was calculated from the slope of GFP fluorescence to optical density during the exponential phase. Error bars indicate the standard error of the mean (n = 9). (For interpretation of the references to colour in this figure legend, the reader is referred to the Web version of this article.)

The integration of the heterologous genes was carried out using a mini-Tn7 integration construct (Zobel et al., 2015), modified to enable marker removal. This provides two main advantages; (I) further genetic modification with the same antibiotic resistance marker is made possible, and (II) application of marker-free strains faces fewer regulatory hurdles in industrial biotechnology. The gentamicin marker in the transposon was replaced by a kanamycin marker flanked by FRT sites, taken from plasmid pBELK (Nikel and de Lorenzo, 2013). A second redundant kanamycin marker was removed from the plasmid backbone. Changing the context of synthetic promoters can significantly affect their activity (Köbbing et al., 2020). Therefore, the resulting constructs were validated with different promoters using *msfGFP* as a reporter gene to ensure that the modifications did not affect the activity of downstream promoters (Fig. 4). Indeed, the activity of P_{em7} was decreased by 70%, in spite of the relatively large distance of 248 bp between the promoter and the modified marker. The activity of the other tested promoters only differed marginally compared to the original construct. In the case of P_{14e} this difference was not significant ($p = 0.2726$), making the generated marker-recycling vector suitable for reliable genomic gene expression.

The influence of genomic expression of P_{14e}-*dcaAKIJP* using the Tn7 construct (designated as "ge") was tested in strain A12.1 (Fig. 3). Strain A12.1ge ($0.33 \pm 0.01\ h^{-1}$) grew at a similar rate as the original evolved strain A12.1p induced with salicylate, while a slightly but significantly ($p = 0.0052$) higher final biomass concentration was obtained with A12.1ge. Apparently, the high constitutive expression with the P_{14e} promoter, possibly combined with better translation initiation and mRNA stability caused by the BCD2 element (Zobel et al., 2015) was sufficient to counteract the reduced copy number of the genomic construct. Given the additional abovementioned advantages of marker-free genomic integration, the influence of the genomic mutations was further characterized using the genomic expression construct.

2.4. Characterization and reverse engineering of genomic mutations for adipate metabolism

Plasmid effects alone cannot explain the differences between A6.1 and A12.1, and even with genomic expression of *dcaAKIJP*, wild-type *P. putida* KT2440 cannot grow on adipate as sole carbon source (Fig. 3). This indicates that the discovered genomic mutations are also foundational to efficient growth on adipate. We therefore set out to characterize individual and combined mutations in a reverse engineering approach, starting with wild-type *P. putida* KT2440 with P_{14e}-*dcaAKIJP* integrated into the genome.

Because the parallels of adipate and phenylacetate degradation start with 2,3-didehydroadipyl-CoA, initial focus was on the influence of the insertion of transposon Tn4652 between *paaFGHIJK* and *paaYX*. The 17-kb transposon was inserted 104 bp upstream of *paaF*, disrupting a putative P_{paaF} promotor. This disruption leads to the emergence of a putative fusion promoter with the native −10 sequence of P_{paaF} and a −35 sequence located in the mosaic end of the transposon. The putative promotor of *paaYX* remains intact (Supporting information 1). To mimic the effect of this insertion, the native promotor was exchanged with the strong synthetic constitutive promoter P_{14g} (Zobel et al., 2015). Possibly, the large transposon insertion separates the promoter from the unknown binding site of the PaaX repressor. In this case, a promoter exchange alone could still be repressed. To test this hypothesis, a knockout of the *paaYX* regulatory genes, as well as a combined promoter insertion and *paaYX* knockout, was performed. The resulting strains all grow at a similar rate of $0.13 \pm 0.00\ h^{-1}$ (Δ*paaYX*, ΔP_{paaF}-*paaYX*::P_{14g}) or $0.14 \pm 0.00\ h^{-1}$ (ΔP_{paaF}::P_{14g}), which is slightly faster than the evolved A6.1p strain but much slower than the reference strain A12.1ge (Fig. 5A). The fact that the knockout of *paaYX*, insertion of P_{14g}, and the combination of both, all enable growth on adipate indicates that either the synthetic promoter P_{14g} is strong enough to drive the transcription of the gene cluster *paaFGHIJK* even in the presence of the PaaX repressor, or that the PaaX binding site overlaps the native P_{paaF} promoter, which was removed during the exchange.

The deletion of *paaYX* and/or promoter exchange upstream of *paaF* enable growth on adipate, but at a lower rate than that of A12.1ge, indicating that further mutations are necessary to completely mimic the evolved phenotype. As described above, an SNP in *psrA* was only found in A12.1. It is likely that this transcriptional regulator represses the two genes *fadB* and *pcaF-II*, which may be involved in the metabolism of 2,3-didehydroadipyl-CoA, the common intermediate between adipate and phenylacetate (Fig. 1). The putative repressive effect of PsrA was confirmed by episomal overexpression, which strongly reduced growth of A12.1 on adipic acid (Fig. S2). Working on the hypothesis that the nonsense mutation disrupted PsrA, the encoding gene was deleted both in the *P. putida* KT2440ge and in the KT2440ge ΔP_{paaF}-*paaYX*::P_{14g} strains. In the wild-type background, the *psrA* knockout leads to weak growth on adipate. The strain grew at a rate of $0.15 \pm 0.01\ h^{-1}$, but only

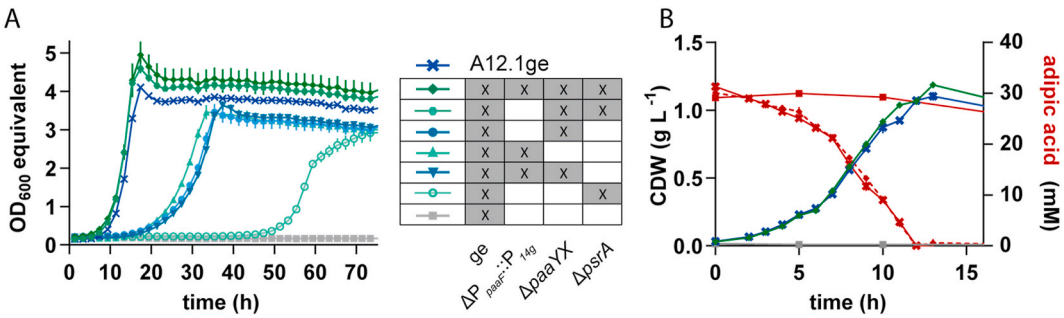

Fig. 5. Characterization of reverse engineered *P. putida* KT2440ge strains. **A**) Growth curves measured with the Growth Profiler. KT2440 genotypes are indicated in table. **B**) Growth curves of *P. putida* KT2440ge ΔP_{paaF}-*paaYX*::P_{14g} Δ*psrA*, KT2440ge, and A12.1ge measured in 500 mL flasks by offline CDW determination. Adipate concentrations were measured by HPLC (red lines). All strains were cultivated in MSM with 30 mM adipate. Error bars indicate the standard error of the mean (n = 3). The abbreviation "ge" denotes genomically integrated marker-free *attTn7*::P_{14e}-*dcaAKIJP*. (For interpretation of the references to colour in this figure legend, the reader is referred to the Web version of this article.)

after a 40-h long lag phase (Fig. 5A). In contrast, *P. putida* KT2440ge ΔP_{paaF}-*paaYX*::P_{14g} Δ*psrA* completely mimicked the growth phenotype of the reference strain A12.1ge (Fig. 5A). This result was verified by growth experiments in shake flasks, which also confirmed full metabolism of adipate by both strains (Fig. 5B). Under these conditions the completely reverse engineered strain grew at a rate of 0.35 ± 0.01 h^{-1}, which is similar to that of A12.1ge (0.34 ± 0.01 h^{-1}). The final biomass reached 1.19 ± 0.01 g L^{-1} after 13 h (Fig. 5), which corresponds to a yield of 0.27 ± 0.00 g_{CDW} $g_{adipate}^{-1}$.

Taken together, these data show that the degradation pathway of adipate in *P. putida* is a hybrid metabolism involving *dcaAKIJP* from *A. baylyi* and partly redundant downstream β-oxidation pathways encoded by *paaFGHIJK* and *fadB/pcaF-II*. Only the combination of the latter two engineering targets resulted in good growth on adipate as sole carbon source. The requirement of this redundancy fits with RB-TnSeq-analysis of *P. putida* growing on medium chain carboxylates and alcohols (Thompson et al., 2020), which could not clearly implicate single enzymes for specific β-oxidation reactions, suggesting that several enzymes may catalyze these steps. Alternatively, the knockout of *psrA* will affect other targets besides *fadB/pcaF-II* (Kang et al., 2008), which may also contribute the improved phenotype.

2.5. Growth of evolved and reverse engineered P. putida strains on other mcl-dicarboxylates

A. baylyi can also grow on longer-chain dicarboxylates besides adipate *via* the DCA pathway (Parke et al., 2001). We therefore analyzed the growth of the evolved and reverse engineered *P. putida* strains on glutaric acid (C_5), pimelic acid (C_7), suberic acid (C_8), azelaic acid (C_9), and sebacic acid (C_{10}) (Fig. 6). With the exception of pimelate, good growth was observed for both the ALE strain A12.1ge and the reverse engineered *P. putida* KT2440ge ΔP_{paaF}-*paaYX*::P_{14g} Δ*psrA*. Wild-type *P. putida* KT2440 only grew on glutaric acid. This C5 dicarboxylate is converted to succinate *via* 2-oxoglutarate, and thus not metabolized *via* β-oxidation (Zhang et al., 2018). The fact that only the evolved and/or engineered strains with the heterologous genes from *A. baylyi* grew on the longer-chain dicarboxylates clearly indicates that they are degraded *via* the same pathway as adipate. In most cases, growth of the strains with the *dca* operon integrated into the genome was similar to that on adipate, although the OD_{max} was higher on sebacate. In contrast, the original ALE-derived strain A12.1p with episomal expression of the *dca* operon showed impaired growth with an extended lag phase on the longer-chain dicarboxylates, further confirming the detrimental effect of the plasmid-based approach. All strains grew slower and reached lower OD_{max} on the longer uneven chain length azelaate and especially on pimelate, indicating a further misregulation of connecting metabolic pathways, possibly at the point of glutaryl-CoA or malonyl-CoA resulting from β-oxidation of these dicarboxylates (Harrison and Harwood, 2005).

2.6. Production of polyhydroxyalkanoates from adipic acid

Engineering of dicarboxylate-metabolizing *P. putida* strains enables the upcycling of these important plastic monomers into value-added compounds. *P. putida* is an efficient producer of many such compounds (Nikel and de Lorenzo, 2018; Schwanemann et al., 2020), among which, polyhydroxyalkanoates (PHAs) are a prominent example (Escapa et al., 2011; Lee et al., 2000; Sun et al., 2007a). Production of PHAs is especially efficient on substrates, which are metabolized *via* β-oxidation to yield acetyl-CoA as primary precursor (Fonseca et al., 2014; Mezzina et al., 2020; Ruiz et al., 2019), making them a promising product for the upcycling of adipate and especially longer-chain dicarboxylates. To test the production of PHAs from adipate, the evolved and reverse engineered strains were cultivated in a nitrogen-limited mineral medium (3x buffered, all cultures reached a final pH of 7.2) with 3.96 g L^{-1} (27.1 mM) adipic acid (Table 2). The evolved *P. putida* KT2440 A12.1ge and the engineered KT2440ge ΔP_{paaF}-*paaYX*::P_{14g} Δ*psrA* reached similar final biomass concentrations. The engineered strain possibly produced more PHA than the evolved strain, but the statistical significance of the difference between these strains is low ($p = 0.086$). Under the conditions tested, the reverse engineered strain produced 25.3 ± 4.2% PHA representing a yield of 9.2% (g g^{-1} of carbon) compared with 6.3% for the evolved strain.

The carbon to PHA yield of the reverse engineered strain compares favorably with previous reported *Pseudomonas* strains grown on 1,4-butandiol (Li et al., 2020) and equimolar terephthalic acid and ethylene glycol (Tiso et al., 2021) both exhibiting a yield of 3.1% (g g^{-1} carbon). The yields are, however, much lower than reported for *P. putida* KT2440 on simple sugars such as glucose under similar flask scale conditions, with greater than 20% yield on a carbon basis (Davis et al., 2013). The addition of fatty acids, as a cofeed strategy, has been shown to increase PHA productivity and yield in the 1,4 butandiol strains, increasing maximal yield to 9.9% with the addition of octanoic acid (Li et al., 2020). A similar strategy could be employed to improve PHA production using adipic acid and consequently improve cost efficiency of the process.

The original evolved strain A12.1p induced with salicylate performed significantly worse, especially with regard to PHA production, which only reached 8.56% of CDW. Unexpectedly, A12.1p performed better without salicylate induction. PHA production was analyzed after 48 h to enable the slower growing uninduced culture to reach maximum production values. However, this also likely caused a longer starvation phase in the other cultures, thereby consuming part of the produced PHA. Previously, the knockout of *psrA* and associated increased β-oxidation activity was shown to cause a shift towards shorter chain lengths in the distribution of PHA monomers (Fonseca et al., 2014). This is likely also the case with the adipate-metabolizing strains. The strain with *psrA* deletion produced a significantly higher fraction of C8 (p =

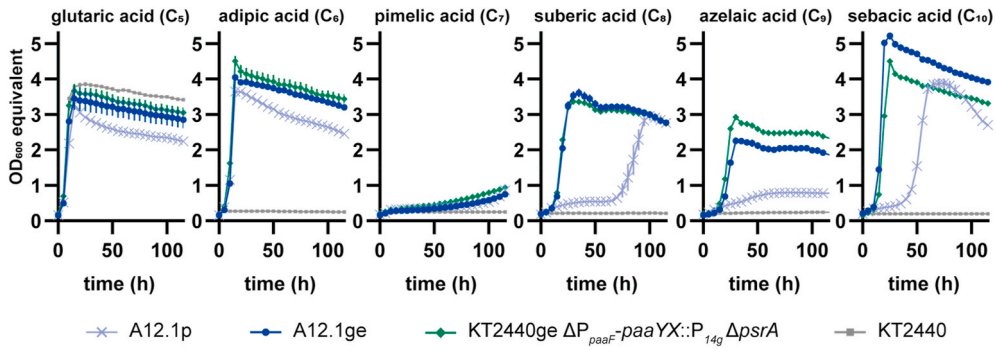

Fig. 6. Growth of evolved and engineered *P. putida* strains on dicarboxylic acids with different chain lengths. All strains were grown in MSM with the indicated carbon sources at a C-molar equivalent to 30 mM adipate. Cultures of A12.1p further contained 0.1 mM salicylate as inducer. The growth curves were measured with a Growth Profiler and the results were converted to an equivalent OD_{600}. Symbols show every 9th data point. Error bars indicate the standard error of the mean (n = 4).

Table 2
Relative monomer composition of PHA polymers produced from adipic acid by evolved and engineered *P. putida* strains.

Strain	CDW (g L^{-1})	PHA (%)	C6 (%)	C8 (%)	C10 (%)	C12 (%)
A12.1p	0.74 ± 0.02	16.8 ± 3.3	3.6 ± 2.6	30.4 ± 1.3	60.8 ± 2.2	5.2 ± 0.1
A12.1p, induced	0.65 ± 0.01	8.6 ± 0.8	4.8 ± 0.4	29.5 ± 0.1	60.0 ± 0.4	5.6 ± 0.8
A12.1ge	0.75 ± 0.01	19.8 ± 0.3	2.8 ± 2.4	33.5 ± 2.3	58.5 ± 2.0	5.2 ± 1.3
KT2440ge ΔP_{paaF}-*paaYX*::P_{14g} Δ*psrA*	0.71 ± 0.03	25.3 ± 4.2	4.6 ± 0.9	28.8 ± 4.6	61.2 ± 6.3	5.4 ± 0.7
KT2440ge ΔP_{paaF}-*paaYX*::P_{14g}	0.69 ± 0.00	22.0 ± 0 4	3.6 ± 0.6	19.8 ± 0.5	70.2 ± 0.3	6.4 ± 0.3

0.029) and possibly also a lower fraction of C10 ($p = 0.069$) monomers than the control strain *P. putida* KT2440ge ΔP_{paaF}-*paaYX*::P_{14g} without Δ*psrA*. Since a narrow monomer distribution is important for PHA polymer properties, this information is valuable to guide efficient upcycling, especially in a mixed culture approach aimed at upcycling complex plastic hydrolysates (Utomo et al., 2020; Nikodinovic et al., 2008).

Table 3
Strains used and generated for adipic acid metabolism.

P. putida strain	Description	Reference
KT2440	Strain derived of *P. putida* mt-2 cured of the pWW0 plasmid	Bagdasarian et al. (1981)
A12.1	KT2440 after evolution on adipate, 12 generations, cured from the evolved plasmid pBNT-*dcaAKIJJP*	This work
A12.1p	Evolved KT2440 strain bearing the evolved plasmid pBNT-*dcaAKIJJP*	This work
A12.1ge	A12.1 after genomic integration of *attTn7*::P_{14e}-*dcaAKIJP* and removal of the resistance marker	This work
KT2440ge	KT2440 after genomic integration of *attTn7*::P_{14e}-*dcaAKIJP* and removal of the resistance marker	This work
KT2440ge ΔP_{paaF}::P_{14g}	Exchange of the natural promoter P_{paaF} for the synthetic P_{14g} promoter	This work
KT2440ge ΔP_{paaF}-*paaYX*::P_{14g}	Exchange of the natural promoter P_{paaF} for the synthetic P_{14g} promoter together with knockout of *paaYX*	This work
KT2440ge Δ*paaYX*	Knockout of *paaYX* without promoter exchange	This work
KT2440ge Δ*psrA*	Knockout of *psrA*	This work
KT2440ge Δ*paaYX* Δ*psrA*	Knockout of *paaYX*, knockout of *psrA*	This work
KT2440ge ΔP_{paaF}-*paaYX*::P_{14g} Δ*psrA*	Exchange of the natural promoter P_{paaF} for the synthetic P_{14g} promoter together with knockout of *paaYX*, knockout of *psrA*	This work

* All strains for molecular biological procedures and the marker recycling experiments are shown in S1.

3. Conclusions

Biological funneling is a powerful approach to convert mixed-plastic hydrolysates into value-added chemicals. This approach requires microbial biotech workhorses that can efficiently metabolize plastic monomers, which was the focus of this study. The substrate spectrum of *P. putida* KT2440 was expanded to include aliphatic dicarboxylic acids. A combination of metabolic engineering and adaptive laboratory evolution enabled and enhanced growth on adipic acid. Genome sequencing and reverse engineering revealed that a hybrid pathway with partially redundant enzyme activities was required for efficient growth. Besides adipate, the resulting strains can also grow on dicarboxylates of other chain length such as suberate, sebacate, and azelaate. This makes them widely applicable for the upcycling of complex hydrolysates derived from different polyesters. Full conversion will also require the metabolism of terminal diols and aromatic dicarboxylates. This can be achieved by defined microbial communities of available strains (Utomo et al., 2020; Li et al, 2019, 2020; Narancic et al., 2021) or by consolidation of multiple monomer-metabolizing pathways into engineered chassis strains. In both cases, a detailed understanding of the underlying biochemical pathways and their regulation is paramount, as was also apparent from the differences in PHA production by strains with and without *psrA* mutation.

4. Experimental procedures

4.1. Strains and culture conditions

The chemicals used in this work were obtained from Carl Roth (Karlsruhe, Germany), Sigma-Aldrich (St. Louis, MO, USA), or Merck (Darmstadt, Germany) unless stated otherwise.

All bacterial strains used in this work are listed in Table 3 or S1. For quantitative microbiology experiments, *P. putida* KT2440 strains were cultivated in three-fold buffered (11.64 g L^{-1} K_2HPO_4, 4.89 g L^{-1} NaH_2PO_4) MSM (Wierckx et al., 2005) unless stated otherwise. Pre-cultures contained 20 mM glucose. For the cultivation with adipic acid, a 300 mM adipic acid stock solution was dissolved 1:10 in MSM to

reach a final concentration of 30 mM. Liquid cultivations were incubated at 30 °C, 200 rpm shaking speed with an amplitude of 50 mm in a Multitron shaker (INFORS, Bottmingen, Switzerland) using 500 mL non-baffled Erlenmeyer flasks with metal caps, containing 50 mL culture volume. For online growth detection without offline sample analysis, a Growth Profiler® 960 (Enzyscreen, Heemstede, The Netherlands) was used. This device analyses cultures in microtiter plates with transparent bottoms by image analysis. Pre-cultures containing 2 mL MSM with 20 mM glucose in 14 mL culture tubes (Greiner bio-one, Frickenhausen, Germany) were cultivated in a Multitron shaker (INFORS) with a 220 rpm shaking speed. Main cultures in 96-well plates with 200 μL volume, using MSM with several concentrations of different carbon sources as indicated, were incubated at 30 °C, 225 rpm shaking speed with an amplitude of 50 mm in the Growth Profiler. Pictures were taken every 30 min.

4.2. Adaptive laboratory evolution

Adaptive laboratory evolution was performed as follows: a preculture of *P. putida* KT2440, cultivated in MSM with 20 mM glucose, was used to inoculate 250 mL clear glass Boston bottles with Mininert valves (Thermo Fisher Scientific, Waltham, MA, USA) containing different concentrations of adipic acid and alternative carbon sources as indicated (starting OD_{600} of 0.01). Unless stated otherwise, serial transfers were reinoculated with a starting OD_{600} of 0.1 after the cultures reached an OD_{600} of at least 0.5. Single colonies were isolated from ALE cultures by streaking samples on LB agar plates.

4.3. Plasmid cloning and strain engineering

Plasmids were assembled by Gibson assembly (Gibson et al., 2009) using the NEBuilder HiFi DNA Assembly Master Mix (New-England Biolabs, Ipswich, MA, USA). Primers were ordered as unmodified DNA oligonucleotides from Eurofins Genomics (Ebersberg, Germany). As polymerase, Q5 High-Fidelity Polymerase was used. Detailed information about utilized primers and plasmid is listed in Tables S2 and S3. For the transformation of DNA assemblies and purified plasmids into competent *E. coli* cells a heat chock protocol was used (Hanahan, 1983). For *P. putida* either conjugational transfer or electroporation were performed as described by Wynands et al. (2018). Knockout strains were obtained using the pEMG system described by Martínez-García and de Lorenzo (2011) with a modified protocol described by Wynands et al. (2018). The integration of heterologous genes from *Acinetobacter baylyi* into the *attTn7*-site of the *P. putida* KT2440 genome was achieved by patch-mating of the *E. coli* donor strain holding the respective pBG-plasmid, the helper strain *E. coli* HB101 pRK2013, *E. coli* DH5α λpir pTNS1 providing the required transposase, and the recipient. Evolved plasmids were isolated from indicated *P. putida* strains using the Monarch Plasmid Miniprep Kit (New- England Biolabs, Ipswich, MA, USA) followed by immediate transformation into *E. coli*.

Plasmids containing FRT-FLP marker recycling were generated from plasmid pBG13 (Zobel et al., 2015), which was used as a template for the origin of transfer *oriT* and origin of replication *oriR6K* containing fragment. A FRT-flanked kanamycin marker was amplified from pBELK (Nikel and de Lorenzo, 2013). Promoters P_{14b} to P_{14g}, BCD2, *msfGFP,* and terminator T0 fragment were amplified from appropriate plasmids pBG14b to pBG14g. A P_{em7} containing fragment was amplified from pBG13 with the same oligonucleotide combination. All fragments were cut out of agarose gels and purified with a DNA Gel Extraction kit (New England Biolabs, Ipswich, Massachusetts, USA). The concentration of purified fragments was measured with a NanoDrop One (Thermo Scientific, Waltham, Massachusetts, USA). Fragments were assembled *via* Gibson Assembly.

The integration of the novel mini-Tn7 vector was done by patch mating as described above. The kanamycin resistance cassette was removed by flippase activity. pBBFLP was transformed *via* electroporation into BGX_FRT_Kan bearing *P. putida* KT2440 strains (X stands for different promoters). Afterwards, cells were plated on LB agar plates containing 30 mg L^{-1} tetracycline to maintain pBBFLP. The growth of clones needed up to two days. Colonies were picked on LB agar plates with and without 50 mg L^{-1} kanamycin to identify clones no longer resistant to kanamycin. Verification was done by colony PCR using One*Taq* 2X Master Mix (New England BioLabs, Ipswich, Massachusetts, USA).

Plasmid inserts, genome integration and gene deletions were confirmed by Sanger sequencing performed by Eurofins Genomics (Ebersberg, Germany).

4.4. Analytical methods

Bacterial growth was monitored as optical density at a wavelength of $\lambda = 600$ nm (OD_{600}) with an Ultrospec 10 Cell Density Meter (GE Healthcare, Little Chalfront, Buckinghamshire, United Kingdom). Cell dry weight values were derived from OD_{600} using a separate calibration. The conversion factor for OD_{600} to CDW is 0.3121. The online analysis of growth using the Growth Profiler was analyzed using the Growth Profiler Control software V2_0_0. Resulting G-values were converted to an equivalent OD_{600} according to the manufacturer's instructions. All growth curves from Growth Profiler experiments of each well was smoothed (window: 5 points) before calculating mean values and standard error of the mean and symbols show every 3rd data point for better visibility, unless stated otherwise. Promoter activities were characterized with a Biolector (M2P Labs, Baesweiler, Germany) in clear bottom 96 well plates (Greiner Bio-One) with a filling volume of 200 μL MSM medium supplemented with 20 mM glucose as sole carbon source. Biomass was measured at 620 nm and GFP fluorescence with ex488 nm/em520 nm. The activity was calculated as a slope of GFP fluorescence over optical density during the exponential phase. A more detailed protocol is described by Köbbing et al. (2020).

4.5. PHA analysis

Single colonies were picked and used to inoculate 2 mL overnight cultures in mineral medium (9 g L^{-1} $Na_2HPO_4{\cdot}12H_2O$, 1.5 g L^{-1} K_2HPO_4, 0.2 g L^{-1} $MgSO_4{\cdot}7\ H_2O$, 1 g L^{-1} NH_4Cl and 1 mL L^{-1} trace elements solution prepared according to Sun et al. (2007b) (Schlegel et al., 1961). The medium was supplemented with 3.96 g L^{-1} of adipic acid (as a sodium salt). Kanamycin and salicylic acid were added to overnight cultures as appropriate. Strains were incubated for 24 h at 30 °C in an orbital shaker at 200 rpm. Overnight cultures were used to inoculate (1% (v/v), inclusion) 250 mL Erlenmeyer flasks containing 50 mL altered mineral medium with reduced nitrogen concentration and a higher buffer capacity (27 g L^{-1} $Na_2HPO_4{\cdot}12\ H_2O$, 4.5 g L^{-1} K_2HPO_4, 0.2 g L^{-1} $MgSO_4{\cdot}7\ H_2O$, 0.25 g L^{-1} NH_4Cl and 1 mL L^{-1} trace elements solution). This medium was supplemented with 3.96 g L^{-1} of adipic acid to achieve a carbon to nitrogen ratio of 30:1. pH was adjusted to 6.5 with 3 M sodium hydroxide. Strains were incubated for 48 h at 30 °C in an orbital shaker at 200 rpm. Flasks were harvested at 48 h for determination of CDW and PHA quantification by acid methanolysis and GC analysis as described in Li et al. (2020).

4.6. Extracellular metabolites

For measuring extracellular metabolites, samples taken from liquid cultivation were centrifuged for 3 min at 17,000×*g* to obtain supernatant for High-Performance Liquid Chromatography (HLPC) analysis using a 1260 Infinity II HPLC equipped with a 1260 Infinity II Refractive Index Detector (Agilent, Santa Clara, California, USA). Analytes were eluted using a 300 × 8 mm organic acid resin column (Metab-AAC, Isera, Düren, Germany) together with a 40 × 8 mm organic acid resin precolumn with 5 mM H_2SO_4 as mobile phase at a flow rate of 0.6 mL min^{-1} at 40 °C.

4.7. Genome sequencing

Genomic DNA for sequencing was isolated through a High Pure PCR Template Preparation Kit (ROCHE life science, Basel, Switzerland). Sequencing was performed by GATC (Konstanz, Germany) using Illumina technology as paired-end reads of 2 × 150 base pairs. The read data (FASTQ files) were processed with the CLC Genomics Workbench software (Qiagen Aarhus A/S) for base quality filtering and read trimming. For each sample, the output was mapped to the GenBank accession AE015451.2 as the *P. putida* KT2440 reference genome sequence and to the pBNT-*dcaAKIJP* plasmid reference sequence. The resulting mappings were used for the gene coverage analysis and the quality-based SNP and structural variant detection with the CLC Genomics Workbench. The detected SNPs were consolidated in one list for sample comparison and inspected regarding their relevance. The mapping was also visualized and inspected with the Integrative Genomics Viewer (IGV) (Thorvaldsdottir et al., 2013).

Sequencing data are deposited in the NCBI Sequence Read Archive under BioProject number PRJNA464914 with accession numbers SRX9220792 for A6.1p and SRX9220793 for A12.1p.

Acknowledgements

We gratefully acknowledge Julia Bockwoldt and Jacqueline Plaster (RWTH Aachen University) for experimental support and María Auxiliadora Prieto (CSIC Madrid) for helpful discussion.

Appendix A. Supplementary data

Supplementary data to this article can be found online at https://doi.org/10.1016/j.ymben.2021.05.001.

Declaration of competing interest

The authors declare no competing interest.

Funding

This project has received funding from the European Union's Horizon 2020 research and innovation programme under Grant Agreements No. 633962 for the project P4SB and No. 870294 for the project MIX-UP.

References

Andrady, A.L., Neal, M.A., 2009. Applications and societal benefits of plastics. Philos. Trans. R. Soc. B Biol. Sci. 364, 1977–1984. https://doi.org/10.1098/rstb.2008.0304.

Aparicio, T., Lorenzo, V., Martínez-García, E., 2019. CRISPR/Cas9-enhanced ssDNA recombineering for *Pseudomonas putida*. Microb. Biotechnol. 12, 1076–1089. https://doi.org/10.1111/1751-7915.13453.

Bagdasarian, M., Lurz, R., Rückert, B., Franklin, F.C.H., Bagdasarian, M.M., Frey, J., Timmis, K.N., 1981. Specific-purpose plasmid cloning vectors II. Broad host range, high copy number, RSF 1010-derived vectors, and a host-vector system for gene cloning in *Pseudomonas*. Gene 16, 237–247. https://doi.org/10.1016/0378-1119(81)90080-9.

Baggi, G., Boga, M.M., Catelani, D., Galli, E., Treccani, V., 1983. Styrene catabolism by a strain of *Pseudomonas fluorescens*. Syst. Appl. Microbiol. 4, 141–147. https://doi.org/10.1016/S0723-2020(83)80042-3.

Barbe, V., Vallenet, D., Fonknechten, N., Kreimeyer, A., Oztas, S., Labarre, L., Cruveiller, S., Robert, C., Duprat, S., Wincker, P., Ornston, L.N., Weissenbach, J., Marlière, P., Cohen, G.N., Médigue, C., 2004. Unique features revealed by the genome sequence of *Acinetobacter* sp. ADP1, a versatile and naturally transformation competent bacterium. Nucleic Acids Res. 32, 5766–5779. https://doi.org/10.1093/nar/gkh910.

Belda, E., van Heck, R.G.A., José Lopez-Sanchez, M., Cruveiller, S., Barbe, V., Fraser, C., Klenk, H.-P., Petersen, J., Morgat, A., Nikel, P.I., Vallenet, D., Rouy, Z., Sekowska, A., Martins dos Santos, V.A.P., de Lorenzo, V., Danchin, A., Médigue, C., 2016. The revisited genome of *Pseudomonas putida* KT2440 enlightens its value as a robust metabolic chassis. Environ. Microbiol. 18, 3403–3424. https://doi.org/10.1111/1462-2920.13230.

Bentley, G.J., Narayanan, N., Jha, R.K., Salvachúa, D., Elmore, J.R., Peabody, G.L., Black, B.A., Ramirez, K., De Capite, A., Michener, W.E., Werner, A.Z., Klingeman, D. M., Schindel, H.S., Nelson, R., Foust, L., Guss, A.M., Dale, T., Johnson, C.W., Beckham, G.T., 2020. Engineering glucose metabolism for enhanced muconic acid production in *Pseudomonas putida* KT2440. Metab. Eng. 59, 64–75. https://doi.org/10.1016/j.ymben.2020.01.001.

Bishop, R.E., 2000. The bacterial lipocalins. Biochim. Biophys. Acta - protein. Struct. Mol. Enzymol. 1482, 73–83. https://doi.org/10.1016/S0167-4838(00)00138-2.

Chae, T.U., Ahn, J.H., Ko, Y.-S., Kim, J.W., Lee, J.A., Lee, E.H., Lee, S.Y., 2020. Metabolic engineering for the production of dicarboxylic acids and diamines. Metab. Eng. 58, 2–16. https://doi.org/10.1016/j.ymben.2019.03.005.

Cheong, S., Clomburg, J.M., Gonzalez, R., 2016. Energy- and carbon-efficient synthesis of functionalized small molecules in bacteria using non-decarboxylative Claisen condensation reactions. Nat. Biotechnol. 34, 556–561. https://doi.org/10.1038/nbt.3505.

Davis, R., Kataria, R., Cerrone, F., Woods, T., Kenny, S., O'Donovan, A., Guzik, M., Shaikh, H., Duane, G., Gupta, V.K., Tuohy, M.G., Padamatti, R.B., Casey, E., O'Connor, K.E., 2013. Conversion of grass biomass into fermentable sugars and its utilization for medium chain length polyhydroxyalkanoate (mcl-PHA) production by *Pseudomonas* strains. Bioresour. Technol. 150, 202–209. https://doi.org/10.1016/j.biortech.2013.10.001.

Escapa, I.F., Morales, V., Martino, V.P., Pollet, E., Avérous, L., García, J.L., Prieto, M.A., 2011. Disruption of β-oxidation pathway in *Pseudomonas putida* KT2442 to produce new functionalized PHAs with thioester groups. Appl. Microbiol. Biotechnol. 89, 1583–1598. https://doi.org/10.1007/s00253-011-3099-4.

Espinosa, M.J.C., Blanco, A.C., Schmidgall, T., Atanasoff-Kardjalieff, A.K., Kappelmeyer, U., Tischler, D., Pieper, D.H., Heipieper, H.J., Eberlein, C., 2020. Toward biorecycling: isolation of a soil bacterium that grows on a polyurethane oligomer and monomer. Front. Microbiol. 11 (404) https://doi.org/10.3389/fmicb.2020.00404.

Fernández, C., Díaz, E., García, J.L., 2014. Insights on the regulation of the phenylacetate degradation pathway from *Escherichia coli*. Environ. Microbiol. Rep 6, 239–250. https://doi.org/10.1111/1758-2229.12117.

Ferrández, A., García, J.L., Díaz, E., 2000. Transcriptional regulation of the divergent *paa* catabolic operons for phenylacetic acid degradation in *Escherichia coli*. J. Biol. Chem. 275, 12214–12222. https://doi.org/10.1074/jbc.275.16.12214.

Fischer, R., Bleichrodt, F.S., Gerischer, U.C., 2008. Aromatic degradative pathways in *Acinetobacter baylyi* underlie carbon catabolite repression. Microbiology 154, 3095–3103. https://doi.org/10.1099/mic.0.2008/016907-0.

Flower, D.R., North, A.C.T., Sansom, C.E., 2000. The lipocalin protein family: structural and sequence overview. Biochim. Biophys. Acta - protein. Struct. Mol. Enzymol. 1482, 9–24. https://doi.org/10.1016/S0167-4838(00)00148-5.

Fonseca, P., de la Peña, F., Prieto, M.A., 2014. A role for the regulator PsrA in the polyhydroxyalkanoate metabolism of *Pseudomonas putida* KT2440. Int. J. Biol. Macromol. 71, 14–20. https://doi.org/10.1016/j.ijbiomac.2014.04.014.

Geyer, R., Jambeck, J.R., Law, K.L., 2017. Production, use, and fate of all plastics ever made. Sci. Adv. 3, e1700782. https://doi.org/10.1126/sciadv.1700782.

Gibson, D.G., Young, L., Chuang, R.-Y., Venter, J.C., Hutchison, C.A., Smith, H.O., 2009. Enzymatic assembly of DNA molecules up to several hundred kilobases. Nat. Methods 6, 343–345. https://doi.org/10.1038/nmeth.1318.

Hanahan, D., 1983. Studies on transformation of *Escherichia coli* with plasmids. J. Mol. Biol. 166, 557–580. https://doi.org/10.1016/S0022-2836(83)80284-8.

Harrison, F.H., Harwood, C.S., 2005. The *pimFABCDE* operon from *Rhodopseudomonas palustris* mediates dicarboxylic acid degradation and participates in anaerobic benzoate degradation. Microbiology 151, 727–736. https://doi.org/10.1099/mic.0.27731-0.

Heipieper, H.J., Neumann, G., Cornelissen, S., Meinhardt, F., 2007. Solvent-tolerant bacteria for biotransformations in two-phase fermentation systems. Appl. Microbiol. Biotechnol. 74, 961–973. https://doi.org/10.1007/s00253-006-0833-4.

Ilves, H., Hõrak, R., Kivisaar, M., 2001. Involvement of ς^S in starvation-induced transposition of *Pseudomonas putida* transposon Tn4652. J. Bacteriol. 183, 5445–5448. https://doi.org/10.1128/JB.183.18.5445-5448.2001.

Kallscheuer, N., Gätgens, J., Lübcke, M., Pietruszka, J., Bott, M., Polen, T., 2017. Improved production of adipate with *Escherichia coli* by reversal of β-oxidation. Appl. Microbiol. Biotechnol. 101, 2371–2382. https://doi.org/10.1007/s00253-016-8033-3.

Kang, Y., Nguyen, D.T., Son, M.S., Hoang, T.T., 2008. The *Pseudomonas aeruginosa* PsrA responds to long-chain fatty acid signals to regulate the *fadBA5* β-oxidation operon. Microbiology 154, 1584–1598. https://doi.org/10.1099/mic.0.2008/018135-0.

Kim, H.T., Kim, J.K., Cha, H.G., Kang, M.J., Lee, H.S., Khang, T.U., Yun, E.J., Lee, D.-H., Song, B.K., Park, S.J., Joo, J.C., Kim, K.H., 2019. Biological valorization of poly (ethylene terephthalate) monomers for upcycling waste PET. ACS Sustain. Chem. Eng. 7, 19396–19406. https://doi.org/10.1021/acssuschemeng.9b03908.

Knott, B.C., Erickson, E., Allen, M.D., Gado, J.E., Graham, R., Kearns, F.L., Pardo, I., Topuzlu, E., Anderson, J.J., Austin, H.P., Dominick, G., Johnson, C.W., Rorrer, N.A., Szostkiewicz, C.J., Copié, V., Payne, C.M., Woodcock, H.L., Donohoe, B.S., Beckham, G.T., McGeehan, J.E., 2020. Characterization and engineering of a two-enzyme system for plastics depolymerization. Proc. Natl. Acad. Sci. 117, 25476–25485. https://doi.org/10.1073/pnas.2006753117.

Köbbing, S., Blank, L.M., Wierckx, N., 2020. Characterization of context-dependent effects on synthetic promoters. Front. Bioeng. Biotechnol. 8 (551) https://doi.org/10.3389/fbioe.2020.00551.

Kohlstedt, M., Starck, S., Barton, N., Stolzenberger, J., Selzer, M., Mehlmann, K., Schneider, R., Pleissner, D., Rinkel, J., Dickschat, J.S., Venus, J., van Duuren, B.J.H., Wittmann, C., 2018. From lignin to nylon: cascaded chemical and biochemical conversion using metabolically engineered *Pseudomonas putida*. Metab. Eng. 47, 279–293. https://doi.org/10.1016/j.ymben.2018.03.003.

Krüger, R., Rakowski, S.A., Filutowicz, M., 2014. Participating Elements in the Replication of Iteron-Containing Plasmids. In: Funnell, B., Phillipps, G. (Eds.),

Plasmid Biology. ASM Press, Washington, DC, USA, pp. 23–45. https://doi.org/10.1128/9781555817732.ch2.
Kruyer, N.S., Peralta-Yahya, P., 2017. Metabolic engineering strategies to bio-adipic acid production. Curr. Opin. Biotechnol. 45, 136–143. https://doi.org/10.1016/j.copbio.2017.03.006.
Kumar, A., von Wolff, N., Rauch, M., Zou, Y.-Q., Shmul, G., Ben-David, Y., Leitus, G., Avram, L., Milstein, D., 2020. Hydrogenative depolymerization of nylons. J. Am. Chem. Soc. 142, 14267–14275. https://doi.org/10.1021/jacs.0c05675.
Kurihara, S., Oda, S., Kato, K., Kim, H.G., Koyanagi, T., Kumagai, H., Suzuki, H., 2005. A novel putrescine utilization pathway involves γ-glutamylated intermediates of *Escherichia coli* K-12. J. Biol. Chem. 280, 4602–4608. https://doi.org/10.1074/jbc.M411114200.
Lee, S.Y., Wong, H.H., Choi, J., Lee, S.H., Lee, S.C., Han, C.S., 2000. Production of medium-chain-length polyhydroxyalkanoates by high-cell-density cultivation of *Pseudomonas putida* under phosphorus limitation. Biotechnol. Bioeng. 68, 466–470. https://doi.org/10.1002/(SICI)1097-0290(20000520)68:4<466::AID-BIT12>3.0.CO;2-T.
Lenzen, C., Wynands, B., Otto, M., Bolzenius, J., Mennicken, P., Blank, L.M., Wierckx, N., 2019. High-yield production of 4-hydroxybenzoate from glucose or glycerol by an engineered *Pseudomonas taiwanensis* VLB120. Front. Bioeng. Biotechnol. 7 https://doi.org/10.3389/fbioe.2019.00130.
Li, W.-J., Jayakody, L.N., Franden, M.A., Wehrmann, M., Daun, T., Hauer, B., Blank, L.M., Beckham, G.T., Klebensberger, J., Wierckx, N., 2019. Laboratory evolution reveals the metabolic and regulatory basis of ethylene glycol metabolism by *Pseudomonas putida* KT2440. Environ. Microbiol. 21, 3669–3682. https://doi.org/10.1111/1462-2920.14703.
Li, W.-J., Narancic, T., Kenny, S.T., Niehoff, P.-J., O'Connor, K., Blank, L.M., Wierckx, N., 2020. Unraveling 1,4-butanediol metabolism in *Pseudomonas putida* KT2440. Front. Microbiol. 11 (382) https://doi.org/10.3389/fmicb.2020.00382.
Magnin, A., Pollet, E., Phalip, V., Avérous, L., 2020. Evaluation of biological degradation of polyurethanes. Biotechnol. Adv. 39 https://doi.org/10.1016/j.biotechadv.2019.107457, 107457.
Martínez-García, E., de Lorenzo, V., 2011. Engineering multiple genomic deletions in Gram-negative bacteria: analysis of the multi-resistant antibiotic profile of *Pseudomonas putida* KT2440. Environ. Microbiol. 13, 2702–2716. https://doi.org/10.1111/j.1462-2920.2011.02538.x.
Meys, R., Frick, F., Westhues, S., Sternberg, A., Klankermayer, J., Bardow, A., 2020. Towards a circular economy for plastic packaging wastes – the environmental potential of chemical recycling. Resour. Conserv. Recycl. 162 https://doi.org/10.1016/j.resconrec.2020.105010, 105010.
Mezzina, M.P., Manoli, M.T., Prieto, M.A., Nikel, P.I., 2020. Engineering native and synthetic pathways in *Pseudomonas putida* for the production of tailored polyhydroxyalkanoates. Biotechnol. J. 2000165 https://doi.org/10.1002/biot.202000165.
Mi, J., Sydow, A., Schempp, F., Becher, D., Schewe, H., Schrader, J., Buchhaupt, M., 2016. Investigation of plasmid-induced growth defect in *Pseudomonas putida*. J. Biotechnol. 231, 167–173. https://doi.org/10.1016/j.jbiotec.2016.06.001.
Narancic, T., Verstichel, S., Reddy Chaganti, S., Morales-Gamez, L., Kenny, S.T., De Wilde, B., Babu Padamati, R., O'Connor, K.E., 2018. Biodegradable plastic blends create new possibilities for end-of-life management of plastics but they are not a panacea for plastic pollution. Environ. Sci. Technol. 52, 10441–10452. https://doi.org/10.1021/acs.est.8b02963.
Narancic, T., Cerrone, F., Beagan, N., O'Connor, K.E., 2020. Recent advances in bioplastics: application and biodegradation. Polymers (Basel) 12 (920). https://doi.org/10.3390/polym12040920.
Narancic, T., Salvador, M., Hughes, G.M., Beagan, N., Abdulmutalib, U., Kenny, S.T., Wu, H., Saccomanno, M., Um, J., O'Connor, K.E., Jiménez, J.I., 2021. Genome analysis of the metabolically versatile *Pseudomonas umsongensis* GO16: the genetic basis for PET monomer upcycling into polyhydroxyalkanoates. Microb. Biotechnol. 1751–7915. https://doi.org/10.1111/1751-7915.13712, 13712.
Nelson, K.E., Weinel, C., Paulsen, I.T., Dodson, R.J., Hilbert, H., Martins dos Santos, V.A.P., Fouts, D.E., Gill, S.R., Pop, M., Holmes, M., Brinkac, L., Beanan, M., DeBoy, R.T., Daugherty, S., Kolonay, J., Madupu, R., Nelson, W., White, O., Peterson, J., Khouri, H., Hance, I., Lee, P.C., Holtzapple, E., Scanlan, D., Tran, K., Moazzez, A., Utterback, T., Rizzo, M., Lee, K., Kosack, D., Moestl, D., Wedler, H., Lauber, J., Stjepandic, D., Hoheisel, J., Straetz, M., Heim, S., Kiewitz, C., Eisen, J., Timmis, K.N., Dusterhoft, A., Tummler, B., Fraser, C.M., 2002. Complete genome sequence and comparative analysis of the metabolically versatile Pseudomonas putida KT2440. Environ. Microbiol. 4, 799–808. https://doi.org/10.1046/j.1462-2920.2002.00366.x.
Nikel, P.I., de Lorenzo, V., 2013. Implantation of unmarked regulatory and metabolic modules in Gram-negative bacteria with specialised mini-transposon delivery vectors. J. Biotechnol. 163, 143–154. https://doi.org/10.1016/j.jbiotec.2012.05.002.
Nikel, P.I., de Lorenzo, V., 2018. *Pseudomonas putida* as a functional chassis for industrial biocatalysis: from native biochemistry to trans-metabolism. Metab. Eng. 50, 142–155. https://doi.org/10.1016/j.ymben.2018.05.005.
Nikel, P.I., Martínez-García, E., de Lorenzo, V., 2014. Biotechnological domestication of *Pseudomonads* using synthetic biology. Nat. Rev. Microbiol. 12, 368–379. https://doi.org/10.1038/nrmicro3253.
Nikodinovic, J., Kenny, S.T., Babu, R.P., Woods, T., Blau, W.J., O'Connor, K.E., 2008. The conversion of BTEX compounds by single and defined mixed cultures to medium-chain-length polyhydroxyalkanoate. Appl. Microbiol. Biotechnol. 80, 665–673. https://doi.org/10.1007/s00253-008-1593-0.
Nurk, A., Tamm, A., Hõrak, R., Kivisaar, M., 1993. In-vivo-generated fusion promoters in *Pseudomonas putida*. Gene 127, 23–29. https://doi.org/10.1016/0378-1119(93)90612-7.
Ornston, L.N., Parke, D., 1976. Properties of an inducible uptake system for β-ketoadipate in *Pseudomonas putida*. J. Biotechnol. 125, 475–488.
Otto, M., Wynands, B., Lenzen, C., Filbig, M., Blank, L.M., Wierckx, N., 2019. Rational engineering of phenylalanine accumulation in *Pseudomonas taiwanensis* to enable high-yield production of trans-cinnamate. Front. Bioeng. Biotechnol. 7 https://doi.org/10.3389/fbioe.2019.00312.
Otto, M., Wynands, B., Marienhagen, J., Blank, L.M., Wierckx, N., 2020. Benzoate synthesis from glucose or glycerol using engineered *Pseudomonas taiwanensis*. Biotechnol. J. 15 https://doi.org/10.1002/biot.202000211, 2000211.
Parales, R.E., Harwood, C.S., 1993. Regulation of the *pcaIJ* genes for aromatic acid degradation in *Pseudomonas putida*. J. Bacteriol. 175, 5829–5838. https://doi.org/10.1128/JB.175.18.5829-5838.1993.
Pardo, I., Jha, R.K., Bermel, R.E., Bratti, F., Gaddis, M., McIntyre, E., Michener, W., Neidle, E.L., Dale, T., Beckham, G.T., Johnson, C.W., 2020. Gene amplification, laboratory evolution, and biosensor screening reveal MucK as a terephthalic acid transporter in *Acinetobacter baylyi* ADP1. Metab. Eng. 62, 260–274. https://doi.org/10.1016/j.ymben.2020.09.009.
Parke, D., Garcia, M.A., Ornston, L.N., 2001. Cloning and genetic characterization of *dca* genes required for β-oxidation of straight-chain dicarboxylic acids in *Acinetobacter* sp. strain ADP1. Appl. Environ. Microbiol. 67, 4817–4827. https://doi.org/10.1128/AEM.67.10.4817-4827.2001.
PlasticsEurope, 2019. Plastics - the facts 2019. PlasticsEurope. Brussels.
Polen, T., Spelberg, M., Bott, M., 2013. Toward biotechnological production of adipic acid and precursors from biorenewables. J. Biotechnol. 167 (2), 75–84. https://doi.org/10.1016/j.jbiotec.2012.07.008.
RameshKumar, S., Shaiju, P., O'Connor, K.E., R B, P, 2020. Bio-based and biodegradable polymers - state-of-the-art, challenges and emerging trends. Curr. Opin. Green Sustain. Chem. 21, 75–81. https://doi.org/10.1016/j.cogsc.2019.12.005.
Rorrer, N.A., Nicholson, S., Carpenter, A., Biddy, M.J., Grundl, N.J., Beckham, G.T., 2019. Combining reclaimed PET with bio-based monomers enables plastics upcycling. Joule 3, 1006–1027. https://doi.org/10.1016/j.joule.2019.01.018.
Ruiz, C., Kenny, S.T., Narancic, T., Babu, R., Connor, K.O., 2019. Conversion of waste cooking oil into medium chain polyhydroxyalkanoates in a high cell density fermentation. J. Biotechnol. 306, 9–15. https://doi.org/10.1016/j.jbiotec.2019.08.020.
Salvachúa, D., Johnson, C.W., Singer, C.A., Rohrer, H., Peterson, D.J., Black, B.A., Knapp, A., Beckham, G.T., 2018. Bioprocess development for muconic acid production from aromatic compounds and lignin. Green Chem. 20, 5007–5019. https://doi.org/10.1039/C8GC02519C.
Sato, K., 1998. A "Green" route to adipic acid: direct oxidation of cyclohexenes with 30 percent hydrogen peroxide. Science 281, 1646–1647. https://doi.org/10.1126/science.281.5383.1646.
Schlegel, H.G., Kaltwasser, H., Gottschalk, G., 1961. A submersion method for culture of hydrogen-oxidizing bacteria: growth physiological studies. Arch. Mikrobiol. 38, 209–222.
Schwanemann, T., Otto, M., Wierckx, N., Wynands, B., 2020. *Pseudomonas* as versatile aromatics cell factory. Biotechnol. J. 15 https://doi.org/10.1002/biot.201900569, 1900569.
Shen, X., Wang, Z., Huang, X., Hu, H., Wang, W., Zhang, X., 2017. Developing genome-reduced *Pseudomonas chlororaphis* strains for the production of secondary metabolites. BMC Genom. 18 (715) https://doi.org/10.1186/s12864-017-4127-2.
Sun, Z., Ramsay, J.A., Guay, M., Ramsay, B., 2007a. Increasing the yield of MCL-PHA from nonanoic acid by co-feeding glucose during the PHA accumulation stage in two-stage fed-batch fermentations of *Pseudomonas putida* KT2440. J. Biotechnol. 132, 280–282. https://doi.org/10.1016/j.jbiotec.2007.02.023.
Sun, Z., Ramsay, J.A., Guay, M., Ramsay, B.A., 2007b. Carbon-limited fed-batch production of medium-chain-length polyhydroxyalkanoates from nonanoic acid by *Pseudomonas putida* KT2440. Appl. Microbiol. Biotechnol. 74, 69–77. https://doi.org/10.1007/s00253-006-0655-4.
Teras, R., Hõrak, R., Kivisaar, M., 2000. Transcription from fusion promoters generated during transposition of transposon Tn4652 is positively affected by integration host factor in *Pseudomonas putida*. J. Bacteriol. 182, 589–598. https://doi.org/10.1128/JB.182.3.589-598.2000.
Teufel, R., Mascaraque, V., Ismail, W., Voss, M., Perera, J., Eisenreich, W., Haehnel, W., Fuchs, G., 2010. Bacterial phenylalanine and phenylacetate catabolic pathway revealed. Proc. Natl. Acad. Sci. U. S. A 107, 14390–14395. https://doi.org/10.1073/pnas.1005399107.
Thompson, M.G., Incha, M.R., Pearson, A.N., Schmidt, M., Sharpless, W.A., Eiben, C.B., Cruz-Morales, P., Blake-Hedges, J.M., Liu, Y., Adams, C.A., Haushalter, R.W., Krishna, R.N., Lichtner, P., Blank, L.M., Mukhopadhyay, A., Deutschbauer, A.M., Shih, P.M., Keasling, J.D., 2020. Fatty acid and alcohol metabolism in *Pseudomonas putida*: functional analysis using random barcode transposon sequencing. Appl. Environ. Microbiol. 86, 1–23. https://doi.org/10.1128/AEM.01665-20.
Thorvaldsdottir, H., Robinson, J.T., Mesirov, J.P., 2013. Integrative Genomics Viewer (IGV): high-performance genomics data visualization and exploration. Brief. Bioinform 14, 178–192. https://doi.org/10.1093/bib/bbs017.
Tiso, T., Narancic, T., Wei, R., Pollet, E., Beagan, N., Schröder, K., Honak, A., Jiang, M., Kenny, S.T., Wierckx, N., Perrin, R., Avérous, L., Zimmermann, W., O'Connor, K., Blank, L.M., 2021. Towards bio-upcycling of polyethylene terephthalate. Metab. Eng. 66, 167–178. https://doi.org/10.1016/j.ymben.2021.03.011.
Tournier, V., Topham, C.M., Gilles, A., David, B., Folgoas, C., Moya-Leclair, E., Kamionka, E., Desrousseaux, M.-L., Texier, H., Gavalda, S., Cot, M., Guémard, E., Dalibey, M., Nomme, J., Cioci, G., Barbe, S., Chateau, M., André, I., Duquesne, S.,

Marty, A., 2020. An engineered PET depolymerase to break down and recycle plastic bottles. Nature 580, 216–219. https://doi.org/10.1038/s41586-020-2149-4.

Tumen-Velasquez, M., Johnson, C.W., Ahmed, A., Dominick, G., Fulk, E.M., Khanna, P., Lee, S.A., Schmidt, A.L., Linger, J.G., Eiteman, M.A., Beckham, G.T., Neidle, E.L., 2018. Accelerating pathway evolution by increasing the gene dosage of chromosomal segments. Proc. Natl. Acad. Sci. 115, 7105–7110. https://doi.org/10.1073/pnas.1803745115.

Utomo, R.N.C., Li, W.-J., Tiso, T., Eberlein, C., Doeker, M., Heipieper, H.J., Jupke, A., Wierckx, N., Blank, L.M., 2020. Defined microbial mixed culture for utilization of polyurethane monomers. ACS Sustain. Chem. Eng. 8, 17466–17474. https://doi.org/10.1021/acssuschemeng.0c06019.

Vardon, D.R., Franden, M.A., Johnson, C.W., Karp, E.M., Guarnieri, M.T., Linger, J.G., Salm, M.J., Strathmann, T.J., Beckham, G.T., 2015. Adipic acid production from lignin. Energy Environ. Sci. 8, 617–628. https://doi.org/10.1039/C4EE03230F.

Vollmer, I., Jenks, M.J.F., Roelands, M.C.P., White, R.J., Harmelen, T., Wild, P., Laan, G. P., Meirer, F., Keurentjes, J.T.F., Weckhuysen, B.M., 2020. Beyond mechanical recycling: giving new life to plastic waste. In: Chemie Int, Angew. (Ed.), 59, pp. 15402–15423. https://doi.org/10.1002/anie.201915651.

Volmer, J., Neumann, C., Bühler, B., Schmid, A., 2014. Engineering of *Pseudomonas taiwanensis* VLB120 for constitutive solvent tolerance and increased specific styrene epoxidation activity. Appl. Environ. Microbiol. 80, 6539–6548. https://doi.org/10.1128/AEM.01940-14.

Wei, R., Tiso, T., Bertling, J., O'Connor, K., Blank, L.M., Bornscheuer, U.T., 2020. Possibilities and limitations of biotechnological plastic degradation and recycling. Nat. Catal. 3, 867–871. https://doi.org/10.1038/s41929-020-00521-w.

Westhues, S., Idel, J., Klankermayer, J., 2018. Molecular catalyst systems as key enablers for tailored polyesters and polycarbonate recycling concepts. Sci. Adv. 4 (8) https://doi.org/10.1126/sciadv.aat9669.

Wierckx, N.J.P., Ballerstedt, H., de Bont, J.A.M., Wery, J., 2005. Engineering of solvent-tolerant *Pseudomonas putida* S12 for bioproduction of phenol from glucose. Appl. Environ. Microbiol. 71, 8221–8227. https://doi.org/10.1128/AEM.71.12.8221-8227.2005.

Wierckx, N., Prieto, M.A., Pomposiello, P., Lorenzo, V., O'Connor, K., Blank, L.M., 2015. Plastic waste as a novel substrate for industrial biotechnology. Microb. Biotechnol. 8, 900–903. https://doi.org/10.1111/1751-7915.12312.

Wilkes, R.A., Aristilde, L., 2017. Degradation and metabolism of synthetic plastics and associated products by *Pseudomonas* sp.: capabilities and challenges. J. Appl. Microbiol. 123, 582–593. https://doi.org/10.1111/jam.13472.

World Economic Forum, Ellen MacArthur Foundation, McKinsey & Company, 2016. The New Plastics Economy: rethinking the future of plastics [WWW Document]. URL. https://www.weforum.org/reports/the-new-plastics-economy-rethinking-the-future-of-plastics.

Wynands, B., Lenzen, C., Otto, M., Koch, F., Blank, L.M., Wierckx, N., 2018. Metabolic engineering of *Pseudomonas taiwanensis* VLB120 with minimal genomic modifications for high-yield phenol production. Metab. Eng. 47, 121–133. https://doi.org/10.1016/j.ymben.2018.03.011.

Wynands, B., Otto, M., Runge, N., Preckel, S., Polen, T., Blank, L.M., Wierckx, N., 2019. Streamlined *Pseudomonas taiwanensis* VLB120 chassis strains with improved bioprocess features. ACS Synth. Biol. 8, 2036–2050. https://doi.org/10.1021/acssynbio.9b00108.

Zhang, M., Gao, C., Guo, X., Guo, S., Kang, Z., Xiao, D., Yan, J., Tao, F., Zhang, W., Dong, W., Liu, P., Yang, C., Ma, C., Xu, P., 2018. Increased glutarate production by blocking the glutaryl-CoA dehydrogenation pathway and a catabolic pathway involving l-2-hydroxyglutarate. Nat. Commun. 9 (2114) https://doi.org/10.1038/s41467-018-04513-0.

Zhao, M., Huang, D., Zhang, X., Koffas, M.A.G., Zhou, J., Deng, Y., 2018. Metabolic engineering of *Escherichia coli* for producing adipic acid through the reverse adipate-degradation pathway. Metab. Eng. 47, 254–262. https://doi.org/10.1016/j.ymben.2018.04.002.

Zobel, S., Benedetti, I., Eisenbach, L., de Lorenzo, V., Wierckx, N., Blank, L.M., 2015. Tn7-based device for calibrated heterologous gene expression in *Pseudomonas putida*. ACS Synth. Biol. 4, 1341–1351. https://doi.org/10.1021/acssynbio.5b00058.